RSC Advances

COMMUNICATION

View Article Online
View Journal | View Issue

One-step transformation of Cu to Cu_2O in alkaline solution†

Cite this: *RSC Adv.*, 2014, **4**, 18616

Received 10th February 2014
Accepted 10th April 2014

DOI: 10.1039/c4ra01174k

www.rsc.org/advances

Jin You Zheng, Thanh-Khue Van, Amol U. Pawar, Chang Woo Kim and Young Soo Kang*

Cu can be directly transformed to Cu_2O before forming CuO in high concentration NaOH aqueous solution by facile surface oxidation reaction without additional oxidant. By using different Cu substrates, pure Cu_2O films with different dominant facets can be obtained.

Copper (Cu), an abundant and ductile metal element with very high electrical and thermal conductivity, has two oxides: cuprous oxide (Cu_2O) and cupric oxide (CuO). Both of them are p-type semiconductors with narrow band gaps of 1.9–2.2 eV and 1.2–1.7 eV, respectively;[1] they are good candidates for solar energy conversion photocatalysts, sensor materials, stable electron sources and optoelectronic device materials. Normally, CuO is dark color since it can absorb all of the visible light even in the infrared range. Although both of them as photocathode materials have poor chemical stabilities for water oxidation and reduction in aqueous solutions, CuO is more unstable than Cu_2O because its redox potential of E_{CuO/Cu_2O} (+0.60 V *vs.* NHE) is more positive than the redox potential of $E_{Cu_2O/Cu}$ (+0.47 V *vs.* NHE);[2] CuO will become Cu_2O followed by Cu_2O reduction to Cu. Therefore, Cu_2O is more valuable than CuO in water splitting area and researchers have focused on improving the stability of Cu_2O by depositing protective layers such as ZnO/Al_2O_3/TiO_2.[2]

Many works have been done for the synthesis of copper oxides regardless of one intractable issue of chemical stability in electrolyte. The copper oxides/hydroxide (CuO, Cu_2O and $Cu(OH)_2$) and Cu can be transformed to one of them by different methods. Cu can be transformed to CuO and Cu_2O by thermal oxidation at high temperature in oxygen atmosphere. Cu_2O is stable at limited ranges of temperature and oxygen pressure and during thermal oxidation of Cu at atmospheric pressure, Cu_2O can be transformed to CuO after a sufficient oxidation time.[3] Musa *et al.*[4] reported that the oxide layer resulting from oxidation at 1050 °C consist only of Cu_2O and those grown below 1040 °C gave mixed oxides of Cu_2O and CuO; they also observed that, in general, the lower temperature of oxidation is, the lower amount of Cu_2O is formed. Choi's group[5] also reported that Cu_2O film can be converted to transparent CuO film by heating in air. For morphology control, CuO wires can also be easily synthesized by heating copper substrates such as Cu TEM grid, foil and conventional electrical wire, even the electrodeposited Cu particle films.[1c,6] Wang's group[7] reported the growth of a scroll-type nanotube structure of $Cu(OH)_2$ arrayed on copper foil at ambient temperature and pressure by surface oxidation of the Cu foil in an alkaline aqueous solution with the oxidant $(NH_4)_2S_2O_8$. Later, Yat Li's group[8] reported that the $Cu(OH)_2$ nanowires obtained *via* the method mentioned above can be converted into Cu_2O nanowires with a small fraction of CuO nanowires by thermal treatment at 450 °C for 1 h in air. Pike *et al.*[9] have shown, using *in situ* time-resolved X-ray diffraction (TR-XRD), that bulk CuO was reduced directly to metallic Cu; and nanoscale CuO can be reduced completely to Cu_2O by isothermal reduction.

As described above, Cu → Cu_2O and/or CuO, Cu_2O → CuO, $Cu(OH)_2$ → Cu_2O and CuO, CuO → Cu_2O can be achieved by thermal oxidation or reduction. However, for the complete conversion of Cu to Cu_2O it requires very high temperature.[4] To the best of our knowledge, there are very few reports on the transformation of Cu to Cu_2O under mild experimental conditions. The Cu surface can be electrochemically oxidized to Cu_2O, CuO and $Cu(OH)_2$ at different potentials in alkaline solution.[10] However, the layer of Cu_2O films was very thin. In addition, Allam and Grimes[11] reported that the various copper oxide nanostructured thin films were synthesized by anodization of Cu foil in aqueous and non-aqueous electrolytes containing hydroxide, chloride and/or fluoride ions at room temperature. Chu *et al.*[12] synthesized CuO crystals with different morphologies such as nanoplates, nanoribbons, nanowires, micro-polyhedrons, mat-like and chrysanthemum-like nanostructures *via* hydrothermal reactions with different types of

Korea Center for Artificial Photosynthesis(KCAP), Department of Chemistry, Sogang University, Seoul 121-742, South Korea. E-mail: yskang@sogang.ac.kr; Fax: +82-2-701-0967

† Electronic supplementary information (ESI) available: Experimental details and characterization (Fig. S1–S7). See DOI: 10.1039/c4ra01174k

surfactants and $(NH_4)_2S_2O_8$ in high concentration of NaOH aqueous solution (5.0 M). Liu *et al.*[13] demonstrated a facile fabrication of flower-like and spherical CuO architectures on Cu substrates by immersing a Cu substrate into low concentrations (30.0 or 65.0 mM) of NaOH and $NH_3 \cdot H_2O$ solutions at 60 °C. Very recently, Luo *et al.*[14] showed that Cu_2O polyhedrons can be directly grown from Cu foil in 0.3 M NaOH at 60 °C. Gao *et al.*[15] have reported an introduction of Cu_2O layer on Cu plate by immersing it into $CuSO_4$ solution. To our surprise, there is no detailed report on the mechanism and process of synthesis and morphological control of pure Cu_2O by simply immersing the different Cu substrates into NaOH solution. Herein, we report a facile process for transformation of Cu foil and Cu film[1c] to pure Cu_2O layer and films without impurity of CuO or $Cu(OH)_2$ in high concentration of NaOH aqueous solution without any surfactants and additives. On the factors influencing the Cu_2O film formation, such as alkali concentration, temperature, reaction time and, especially, the most critical factor for Cu substrates with different dominant crystal facets have been discussed.

It is known that the relation of the surface energy (γ) of bulk face-centered cubic (fcc) metals is $\gamma_{111} < \gamma_{100} < \gamma_{110}$.[16] The relation of the surface energy of fcc Cu is also a decreasing order as $\gamma_{Cu(111)} < \gamma_{Cu(100)} < \gamma_{Cu(110)}$.[17] Therefore, the different dominant facets of bulk fcc Cu in a solution will have different adsorption–desorption rate and chemical reaction rate. Herein, three different kinds of Cu foil and Cu/FTO film substrates, as their XRD patterns indexed as fcc-phase copper (JCPDS no. 65-9743) shown in Fig. 1(a) and 4(a2), were conducted for the experiments. The peak intensity ratios of $I_{(111)}/I_{(200)}$ and $I_{(220)}/I_{(200)}$ are 0.66 and 0.39 for Cu_1, 0.04 and 0.13 for Cu_2 and 2.92 and 0.52 for Cu/FTO, respectively. A typical experimental process of one-step transformation of Cu to Cu_2O was conducted by immersion of Cu substrates in NaOH aqueous solution at 80 °C for 1 h and kept at room temperature (24 °C) during various aging times, such as 14 h, as shown in Scheme 1(a). After the reactions, the as-synthesized film was washed by deionized water, ethanol and then dried under N_2 gas flow. The brownish red colored film was covered on the surface of Cu foil and the transparent film with darker orange color was formed on FTO glass as shown in Fig. 1(b). According to the description in ref. 12, 13 and 18, the possible reaction processes are given as

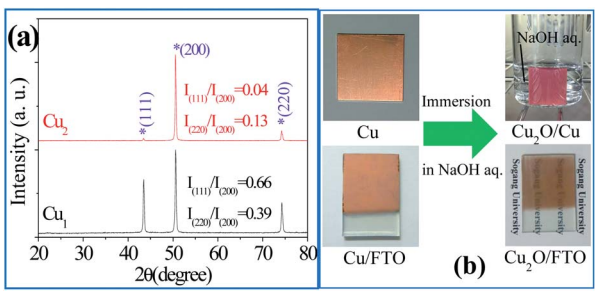

Fig. 1 (a) XRD patterns of two different copper foils (Cu_1 and Cu_2) with different intensity ratios of crystal facets; (b) the photographs to show the typical experimental processes of the one-step formation of Cu_2O film on Cu foil and FTO coated glass surface by immersion in NaOH solution.

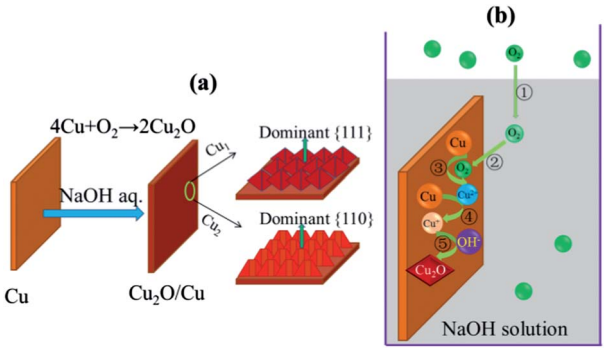

Scheme 1 Schematic illustration of (a) the preparation process and (b) the growth mechanism.

following (see the detail explanation; ESI†): Cu foil or Cu/FTO can continuously release Cu^{2+} ions into NaOH solution by the naturally-dissolved O_2 oxidization

$$2\,Cu + O_2 + 2H_2O \rightarrow 2Cu^{2+} + 4OH^- \quad (1)$$

Then, some of Cu^+ ions can be produced by the process of

$$Cu^{2+} + Cu \rightarrow 2Cu^+ \quad (2)$$

The maximum concentration of $[Cu^+]$ is determined by the equation of

$$\log [Cu^+]_{max} = -0.84 - pH \text{ (ref. 18c)} \quad (3)$$

If the real concentration of Cu^+ exceeds the $[Cu^+]_{max}$ given by eqn (3), the following process will be done.

$$2Cu^+ + 2OH^- \rightarrow Cu_2O + H_2O \quad (4)$$

This process is similar to that Cu^{2+} ions can be reduced to Cu^+ ions by Cu plate then form Cu_2O layer on Cu surface through *in situ* redox reaction according to eqn (5) in the ref. 15.

$$Cu^{2+} + Cu + H_2O \rightarrow Cu_2O + 2H^+ \quad (5)$$

The transformation of Cu to Cu_2O in our experiment can be carried out by the net reaction as follows:

$$4Cu + O_2 \rightarrow 2Cu_2O \quad (6)$$

In summary, we present a growth mechanism of Cu_2O from Cu in high concentration alkaline solution with 5 steps as shown in Scheme 1(b). Step 1, the O_2 in air is dissolved in alkaline solution. Step 2, the dissolved O_2 is adsorbed on the surface of Cu. Steps 3, the Cu atoms in surface are oxidized to Cu^{2+} ions by the adsorbed O_2 as the reaction (1). Step 4, the Cu^{2+} ions can be reduced to Cu^+ ions by neighboring Cu atoms during very short time as the reaction (2). Step 5, the Cu^+ ions will react with OH^- in solution to form Cu_2O nucleation sites and H_2O molecules are released from the Cu surface as the reaction (4). The obtained Cu_2O nucleation sites will grow according to reaction time. Finally, the nano/micro-sized Cu_2O

crystals can be formed. In the whole Cu_2O growth process, steps 3 to 5 are happened *in situ* on Cu surface. The step 2 is a key to open the next reactions, which depends on the adsorption of O_2 by Cu surface. Therefore, the surface property of Cu substrate is a critical factor for the experiment.

The XRD pattern of Cu_2O/Cu_1 can be fully indexed to a pure cubic phase with space group of $Pn\bar{3}m$ (no. 224) of Cu_2O (JCPDS no. 65-3288) except the peaks of Cu_1 substrate as shown in Fig. 2(a). The physicochemical properties of crystals such as adsorption, catalytic reactivity and selectivity *etc.*, significantly depend on the surface atomic configuration and the degree of exposure of reactive crystal facet.[19] The dominant crystal facet of Cu_2O/Cu_1 is (111). The corresponding SEM image as shown in Fig. 2(b) indicates that the compact and homogenous Cu_2O octahedrons particle film is covered on the Cu_1 foil. The low magnification SEM images, TEM image and SEAD pattern in Fig. S1 (ESI†) further demonstrate that the Cu_2O octahedron film with the average particle size of less than 1.5 μm is in large area scale and the particles are single crystalline. Since the surface energy order is $\gamma_{Cu(111)} < \gamma_{Cu(100)} < \gamma_{Cu(110)}$ as previously stated, the Cu_1 with high $I_{(111)}/I_{(200)}$ needs longer reaction time (3 days) to form regular Cu_2O octahedron film.

In contrast, it is assumed that the Cu substrate with very low $I_{(111)}/I_{(200)}$ should have shorter reaction time to form Cu_2O film by immersion in NaOH aqueous solution. To verify the assumption, the Cu_2 substrates were used for experiments. The Cu_2 foil was immersed in a 4.0 M hot NaOH aqueous solution of 80 °C and then kept at room temperature for 14 h. As shown in Fig. 3(a), the compact imperfect 26-facet polyhedral architecture (a perfect one with exposed 8 {111}, 6 {100} and 12 {110} facets as the inset shown in Fig. 3(a)) was obtained.[20] The size of particles is in the range of several microns and the thickness of film is *ca.* 3.5 μm as shown in Fig. S2 (ESI†). The {110} facets are exposed inhomogeneously. The dominant facet is {200} as shown in XRD pattern of Fig. 3(b). The purity of the as-obtained Cu_2O was further identified by X-ray photoelectron spectroscopy (XPS). Normally, the CuO and $Cu(OH)_2$ can be characterized by intense Cu(2p) XPS shake-up satellites and a broad O(1s) peak; Cu_2O and metallic Cu show weaker/no Cu(2p) satellites and a narrower O(1s) peak.[21]

Unfortunately, it is difficult to distinguish the Cu_2O and the metallic Cu by XPS since their Cu(2p) binding energies are similar.[22] However, herein, we just need to ensure non-existences of CuO and $Cu(OH)_2$ by XPS. Some very weaker shake-up satellites peaks rather than intense satellites peaks indicate that there is no impurities of CuO and $Cu(OH)_2$ in our samples as shown in Fig. 3(c). Considering the depth of detection of XPS (~1 to 10 nm), the peaks of $Cu(2p_{3/2})$ at 932.6 eV and $Cu(2p_{1/2})$ at 952.4 eV can be attributed to Cu_2O.[22] The corresponding O(1s) XPS spectra show two peaks at 530.3 and 531.5 eV, attributed to Cu_2O and surface hydroxide (–OH).[23] The surface hydroxide comes from the adsorbed and/or residual NaOH on the surface of Cu_2O. The pure Cu_2O crystals can also be obtained by immersing Cu_2 foils at different concentrations of NaOH solution even at room temperature (24 °C) as shown in Fig. S3 and S4.† At low concentration (2.0 M), the size of particles is relatively decreased; when the concentration was increased, the films become loose and sparse. At room temperature, the Cu_2O particles are much irregular and cannot be formed at very high concentration (8.0 M). The Cu_2O/Cu can be further oxidized to CuO/Cu as the immersion time was extended as shown in Fig. S5.† In general, the products can be affected by several parameters such as temperature, NaOH concentration and reaction time.

The photoelectrochemical photocurrent switching (PEPS) effect,[1c,24] which can switch photocurrent polarity by changing photoelectrode potential, was observed with Cu_2O/Cu_2 sample as shown in Fig. 3(e). The cathodic photocurrent gradually decreases as the applied potential is swept from −0.7 V to the

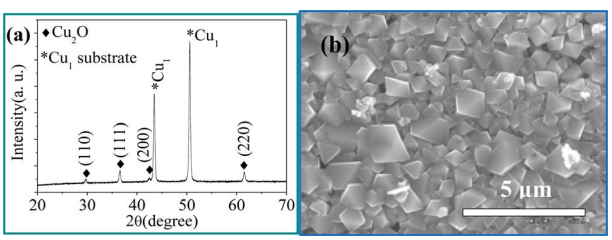

Fig. 2 (a) XRD pattern and (b) SEM image of Cu_2O/Cu_1 obtained by adding Cu_1 foils in 20 ml 4 M NaOH aqueous solution followed by heating at 80 °C for around 1 h and then kept at room temperature for 4 days.

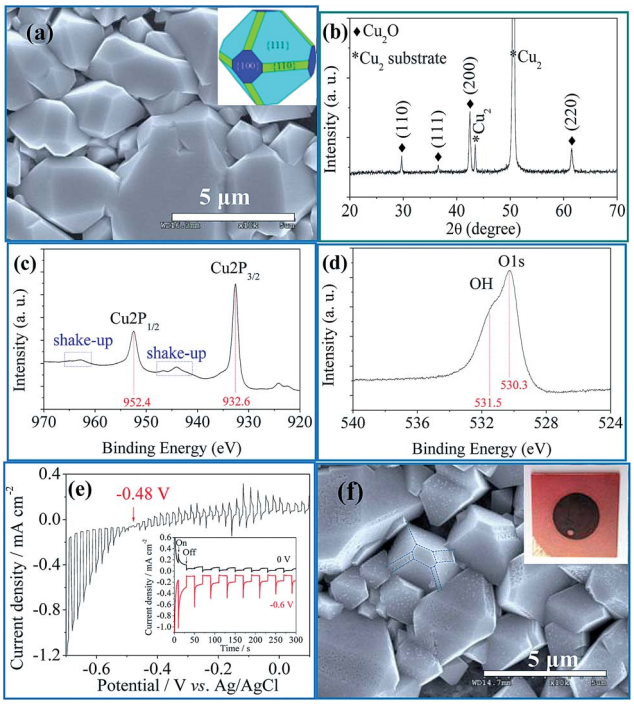

Fig. 3 (a) SEM image, (b) XRD pattern and XPS spectra of (c) Cu2p and (d) O1s, (e) photocurrent and photoresponse curves under 1 sun illumination of Cu_2O/Cu_2 obtained by adding Cu_2 foils in 20 ml 4.0 M NaOH solution with initial temperature of 80 °C and then kept at room temperature for 14 h. (f) SEM images of Cu_2O/Cu_2 after checking (e). The inset in (a) is a perfect 26-facet polyhedral architecture with exposed {111} × 8, {100} × 6 and {110} × 12 facets. The inset of (f) is the photograph of Cu_2O/Cu_2 film after checking (e).

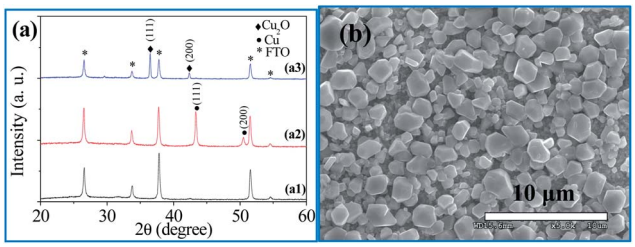

Fig. 4 (a) XRD patterns of (a1) bared FTO, (a2) Cu/FTO and (a3) Cu_2O/FTO; (b) SEM image of Cu_2O/FTO obtained by immersing Cu/FTO substrate into 20 ml 4.0 M NaOH solution followed by heating at 80 °C for around 1 h and then kept at room temperature for 5 days.

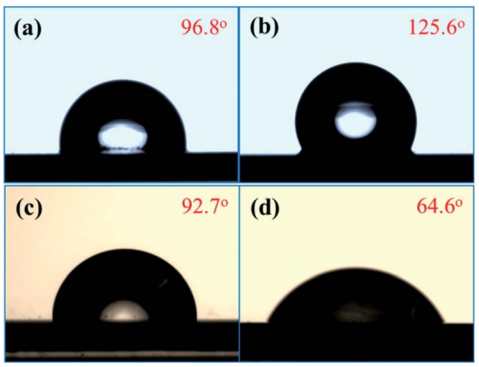

Fig. 5 Contact angle measurement results of (a) bare Cu_1 foil, (b) Cu_2O/Cu_1 film, (c) bare Cu_2 foil and (d) Cu_2O/Cu_2 film.

positive direction and is converted to anodic photocurrent at −0.48 V. Herein, the performance of the current-potential under chopped light illumination indicates that Cu/Cu_2O and Cu_2O/electrolyte Schottky type junctions exist in the Cu/Cu_2O/electrolyte system. Similar results have been investigated earlier in the Ti/Cu_2O/electrolyte,[25] ITO/Cu_2O/electrolyte[26] and ITO/Cu_2O/Cu_xS[27] systems. When the potential is in the range of −0.7 to −0.48 V, the Cu/Cu_2O junction is dominant and therefore a p-type photosignal (cathodic photocurrent) is produced; when the potential is in the range of −0.48 to +0.1 V, the Cu_2O/electrolyte junction becomes dominant and therefore a n-type photosignal (anodic photocurrent) is obtained.[25] The anodic and cathodic photocurrents were observed by photoresponses at 0 V and −0.6 V, respectively, as the inset in Fig. 3(e). The cathodic photocurrent decreased gradually as time was increased under −0.6 V. It indicates that the film is not so stable. After the photocurrent and photoresponse checking, the color of the surface of film, which was exposed in electrolyte, was changed to dark as shown in the inset in Fig. 3(f); it indicates that Cu_2O was reduced to Cu on the surface as a similar result reported by Paracchine *et al.*[2] As shown in the SEM image in Fig. 3(f) and S6 (ESI†), the {110} crystal facets are partially dissolved while the others are stable. Many nano-sized Cu particles are deposited onto the {111} facets. This process is a decomposition–redeposition process. The relative surface energies of Cu_2O crystals are in the order of $\gamma\{111\} < \gamma\{100\} < \gamma\{110\}$ and the order of photocatalytic activity of facets in Cu_2O is {110} > {111} > {100}.[28] Therefore, the {110} facet possesses the highest surface energy and is the most photoactive facet here. The {110} should be the most active facet for the reaction such as water splitting under light illumination. However, the {110} facet is the most unstable facet. For comparison, the Cu/FTO substrate with high $I_{(111)}/I_{(200)}$ ratio of 2.92 was chosen for experiment. After 5 day immersion, the Cu films can be completely transformed to Cu_2O as the XRD patterns shown in Fig. 4(a). The dominant crystal facet is (111). However, the film is composed of crystals of irregular polyhedron particles as shown in Fig. 4(b). The Cu_2O/FTO is not perfect because the Cu/FTO is composed of Cu particles rather than continuous and compact film as shown in Fig. S7 (ESI†).

To show further potential applications, the hydrophobicity properties of two kinds of Cu_2O films in Fig. 2(b) and 3(a) were tested *via* water contact angle as shown in Fig. 5. It is found that the surfaces of Cu_1 (Fig. 5(a)) and Cu_2 (Fig. 5(c)) substrates are hydrophobic with similar water contact angle of 96.8 ± 3° and 92.7 ± 3°, respectively. After formed Cu_2O film on the surface of Cu substrates, the surface of Cu_2O/Cu_1, with water contact angle of 125.6 ± 2°, is more hydrophobic than the bare Cu_1 substrate. In contrast, the Cu_2O/Cu_2 presents hydrophilic property with water contact angle of 64.6 ± 2°. In theory, the hydrophobic solid surface has low surface energy and the hydrophilic solid surface has high surface energy. Since the relative surface energies of Cu_2O crystals are in the order of $\gamma\{111\} < \gamma\{100\}$, the water contact angle of Cu_2O/Cu_1 film with dominant {111} facets should be larger than that of Cu_2O/Cu_2 film with dominant {100} facets. This is matched with the experimental results regardless of the other factors such as the morphology and the surface adsorption.

In summary, Cu can be directly transformed to Cu_2O before the formation of CuO in high concentrated NaOH aqueous solution by facile immersion process without any additional oxidant. According to the different type of Cu substrates, the different dominant Cu_2O films can be obtained. The process of Cu oxidation in high concentration of aqueous NaOH is from Cu to Cu_2O, and then Cu_2O to CuO as the immersion time is prolonged. Further work will be reported for the better understanding of the mechanism of growth in the following report. However, this work gives a good way to convert Cu particle or Cu film to crystalline Cu_2O particle or film and it can be a facile way to synthesize Cu_2O films.

Acknowledgements

This work was supported by the Korea Center for Artificial Photosynthesis (KCAP) located in Sogang University funded by the Minister of Science, ICT and Future Planning (MSIP) through the National Research Foundation of Korea (no. 2009-0093885), and the Brain Korea 21 Plus Project 2014.

Notes and references

1 (*a*) G. Filipic and C. Cvelbar, *Nanotechnology*, 2012, **23**, 194001; (*b*) J. Y. Zheng, A. P. Jadhav, G. Song, C. W. Kim and Y. S. Kang, *Thin Solid Films*, 2012, **524**, 50; (*c*)

J. Y. Zheng, G. Song, C. W. Kim and Y. S. Kang, *Electrochim. Acta*, 2012, **69**, 340.
2 A. Paracchine, V. Laporte, K. Sivula, M. Gratzel and E. Thimsen, *Nat. Mater.*, 2011, **10**, 456.
3 (*a*) A. Roos and B. Karlson, *Sol. Energy Mater.*, 1983, **7**, 467; (*b*) A. Roos, T. Chibuye and B. Karlson, *Sol. Energy Mater.*, 1983, **7**, 453.
4 A. O. Musa, T. Akomolafe and M. J. Carter, *Sol. Energy Mater. Sol. Cells*, 1998, **51**, 305.
5 K. E. R. Brown and K.-S. Choi, *Chem. Commun.*, 2006, 3311.
6 X. Jiang, T. Herricks and Y. Xia, *Nano Lett.*, 2002, **2**, 1333.
7 W. Zhang, X. Wen, S. Yang, Y. Berta and Z. L. Wang, *Adv. Mater.*, 2003, **15**, 822.
8 F. Qian, G. Wang and Y. Li, *Nano Lett.*, 2010, **10**, 4686.
9 J. Pike, S. W. Chan, F. Zhang, X. Wang and J. Hanson, *Appl. Catal., A*, 2006, **303**, 273.
10 (*a*) H. M. Hollmark, P. G. Keech, J. R. Vegelius, L. Werme and L.-C. Duda, *Corros. Sci.*, 2012, **54**, 85; (*b*) J. Wu, X. Li, B. Yadian, H. Liu, S. Chun, B. Zhang, K. Zhou, C. L. Gan and Y. Huang, *Electrochem. Commun.*, 2013, **26**, 21.
11 N. K. Allam and C. A. Grimes, *Mater. Lett.*, 2011, **65**, 1949.
12 Y. Liu, Y. Chu, M. Y. Li and L. H. Dong, *J. Mater. Chem.*, 2006, **16**, 192.
13 J. Liu, X. Huang, Y. Li, K. M. Sulieman, X. He and F. Sun, *J. Mater. Chem.*, 2006, **16**, 4427.
14 Z. J. Luo, T. T. Han, L. L. Qu and X. Y. Wu, *Chin. Chem. Lett.*, 2012, **23**, 953.
15 T. Gao, Y. Wang, K. Wang, X. Zhang, J. Dui, G. Li, S. Lou and S. Zhou, *ACS Appl. Mater. Interfaces*, 2013, **5**, 7308.
16 P. I. Wang, Y. P. Zhao, G. C. Wang and T. M. Lu, *Nanotechnology*, 2004, **15**, 218.
17 (*a*) B. D. Todd and R. M. Lynden-Bell, *Surf. Sci.*, 1993, **281**, 191; (*b*) S. G. Wang, E. K. Tian and C. W. Lung, *J. Phys. Chem. Solids*, 2000, **61**, 1295.
18 (*a*) W. Z. Wang, O. K. Varghese, C. M. Ruan, M. Paulose and C. A. Grimes, *J. Mater. Res.*, 2003, **18**, 2756; (*b*) S. Sun, H. Zhang, X. Song, S. Liang, C. Kong and Z. Yang, *CrystEngComm*, 2011, **13**, 6040; (*c*) A. Survila, P. Kalinauskas and I. Valsiūnas, *Russ. J. Electrochem.*, 2002, **38**, 1068.
19 S. Liu, J. Yu and M. Jaroniec, *Chem. Mater.*, 2011, **23**, 4085.
20 B. Heng, T. Xiao, W. Tao, X. Hu, X. Chen, B. Wang, D. Sun and Y. Tang, *Cryst. Growth Des.*, 2012, **12**, 3998.
21 (*a*) M. Komarneni, J. Shan, A. Chakradhar, E. Kadossov, S. Cabrini and U. Burghaus, *J. Phys. Chem. C*, 2012, **116**, 5792; (*b*) M. C. Biesinger, L. W. M. Lau, A. R. Gerson and R. St. C. Smart, *Appl. Surf. Sci.*, 2010, **257**, 887.
22 A. Radi, D. Pradhan, Y. Sohn and K. T. Leung, *ACS Nano*, 2010, **4**, 1553.
23 J. E. Yourey and B. M. Bartlett, *J. Mater. Chem.*, 2011, **21**, 7651.
24 K. Szaciłowski and W. Macyk, *Chimia*, 2007, **61**, 831.
25 R. P. Wijesundera, M. Hidaka, K. Koga, M. Sakai and W. Siripala, *Thin Solid Films*, 2006, **500**, 241.
26 W. Siripala, *J. Natl. Sci. Counc. Sri Lanka*, 1995, **23**, 49.
27 R. P. Wijesundera, L. D. R. D. Perera, K. D. Jayasuriya, W. Siripala, K. T. L. De Silva, A. P. Samantilleka and I. M. Darmadasa, *Sol. Energy Mater. Sol. Cells*, 2000, **61**, 277.
28 (*a*) Y. Zhang, B. Deng, T. R. Zhang, D. M. Gao and A. W. Xu, *J. Phys. Chem. C*, 2010, **114**, 5073; (*b*) S. Sun, X. Song, Y. Sun, D. Deng and Z. Yang, *Catal. Sci. Technol.*, 2012, **2**, 925.

